YvcI from *Bacillus subtilis* has *in vitro* RNA pyrophosphohydrolase activity

Jens Frindert[‡], Masroor Ahmad Kahloon[‡], Yaqing Zhang[‡], Yasar Luqman Ahmed[§], Irmgard Sinning[§], and Andres Jäschke[‡1]

Received for publication, October 14, 2019, and in revised form, November 15, 2019 Published, Papers in Press, November 18, 2019, DOI 10.1074/jbc.RA119.011485

From the [‡]Institute of Pharmacy and Molecular Biotechnology and the [§]Heidelberg University Biochemistry Center, Heidelberg University, D-69120 Heidelberg, Germany

Edited by Karin Musier-Forsyth

RNA degradation is one of several ways for organisms to regulate gene expression. In bacteria, the removal of two terminal phosphate moieties as orthophosphate (*Bacillus subtilis*) or pyrophosphate (*Escherichia coli*) triggers ribonucleolytic decay of primary transcripts by 5′-monophosphate–dependent ribonucleases. In the soil-dwelling firmicute species *B. subtilis*, the RNA pyrophosphohydrolase BsRppH, a member of the Nudix family, triggers RNA turnover by converting primary transcripts to 5′-monophospate RNA. In addition to BsRppH, a source of redundant activity in *B. subtilis* has been proposed. Here, using recombinant protein expression and *in vitro* enzyme assays, we provide evidence for several additional RNA pyrophosphohydrolases, among them MutT, NudF, YmaB, and YvcI in *B. subtilis*. We found that *in vitro*, YvcI converts RNA 5′-di- and triphosphates into monophosphates in the presence of manganese at neutral to slightly acidic pH. It preferred G-initiating RNAs and required at least one unpaired nucleotide at the 5′-end of its substrates, with the 5′-terminal nucleotide determining whether primarily ortho- or pyrophosphate is released. Exchanges of catalytically important glutamate residues in the Nudix motif impaired or abolished the enzymatic activity of YvcI. In summary, the results of our extensive *in vitro* biochemical characterization raise the possibility that YvcI is an additional RNA pyrophosphohydrolase in *B. subtilis*.

In bacteria, gene expression is tightly controlled because an ever-changing environment requires rapid adaption of the microbes to survive. Various levels of control exist, among them mRNA turnover. In living organisms, the half-lives of individual transcripts differ tremendously, affecting protein biosynthesis accordingly. However, the molecular properties that influence the stability of individual mRNAs are still not fully understood.

In prokaryotes, mRNAs are typically protected from ribonucleolytic decay by a triphosphate group (ppp)[2] at their 5′-terminus and a stem-loop structure at their 3′-terminus. In the γ-proteobacterium *Escherichia coli*, the major RNase in mRNA turnover is endonuclease RNase E, and two pathways exist as to how RNA degradation is initiated. In the direct-access pathway, degradation starts with endoribonucleolytic attack, whereas in the 5′-end-dependent pathway, the 5′-ppp of the RNA has first to be converted into a monophosphate (p) by the RNA pyrophosphohydrolase RppH (1). RppH cuts between the α and β phosphates of the 5′-ppp releasing pyrophosphate (pp_i), whereby a small portion is released as orthophosphate (p_i) *in vitro* (2). Recently, diphosphorylated RNAs (pp-RNAs) were found in *E. coli*, and RppH prefers them over their triphosphorylated precursors (3). RppH requires at least two unpaired nucleotides at the 5′-end of its RNA substrates. Thereby, the 5′-terminal sequence is of minor importance, although transcripts initiating with A are slightly preferred over messages starting with G. The same applies for RNAs with a purine at position +2 (4). Because of its nonselective substrate specificity, RppH might be the only hydrolase of this kind in *E. coli* (5).

In the firmicute *Bacillus subtilis*, mRNA turnover differs from *E. coli*. Major differences are the presence of 5′-to-3′-exoribonucleases, RNase J1 and J2, and the absence of an RNase E homolog, which seems to be functionally replaced by the 5′-p-dependent endoribonuclease RNase Y (6). RNase Y or RNase J1 initiate the direct-access pathway by endonucleolytic cleavage of the mRNA. The 5′-terminal cleavage product is subjected to decay by 3′-to-5′-exonucleases, whereas the 3′-fragment, which is 5′-monophosphorylated, is degraded by RNase J1. The activity of RNase J1 is stimulated by 5′-p-ends and impeded by 5′-ppp (7). Moreover, the enzyme needs a single-stranded 5′-RNA-terminus of at least nine nucleotides for maximal processivity (8). In the 5′-dependent pathway, conversion of 5′-ppp-RNA into 5′-p-RNA is catalyzed by *B. subtilis* RNA pyrophosphohydrolase BsRppH (*rppH*), which removes the γ and β phosphates as orthophosphate (9). Upon phosphate removal, the p-RNA is degraded by RNase J1 (10) or RNase Y. BsRppH shows a much more pronounced substrate specificity than RppH from *E. coli*. This Nudix hydrolase is strongly impeded when the 5′-terminus of the RNA is sequestered by base pairing (9) and requires at least two unpaired nucleotides at the 5′-end (11). In addition, it slightly prefers substrates initiating with A over G. Moreover, the enzyme was reported to strongly prefer a G at position +2 of the RNA (~5–10-fold according to Ref. 12 or complete loss of activity upon mutation

This work was supported by Baden-Württemberg Stiftung Grant BWST_NCRNA_045] and in part by Deutsche Forschungsgemeinschaft Priority Program SPP 1784 Grant Ja794/10-1. The authors declare that they have no conflicts of interest with the contents of this article.

This article contains supporting text, Tables S1–S4, and Figs. S1–S6.

[1] To whom correspondence should be addressed. Tel.: 49-6221-544851; Fax: 49-6221-546430; E-mail: jaeschke@uni-hd.de.

[2] The abbreviations used are: ppp, triphosphate group; p, monophosphate; pp_i, pyrophosphate; p_i, orthophosphate; h, human; PEI, polyethyleneimine.

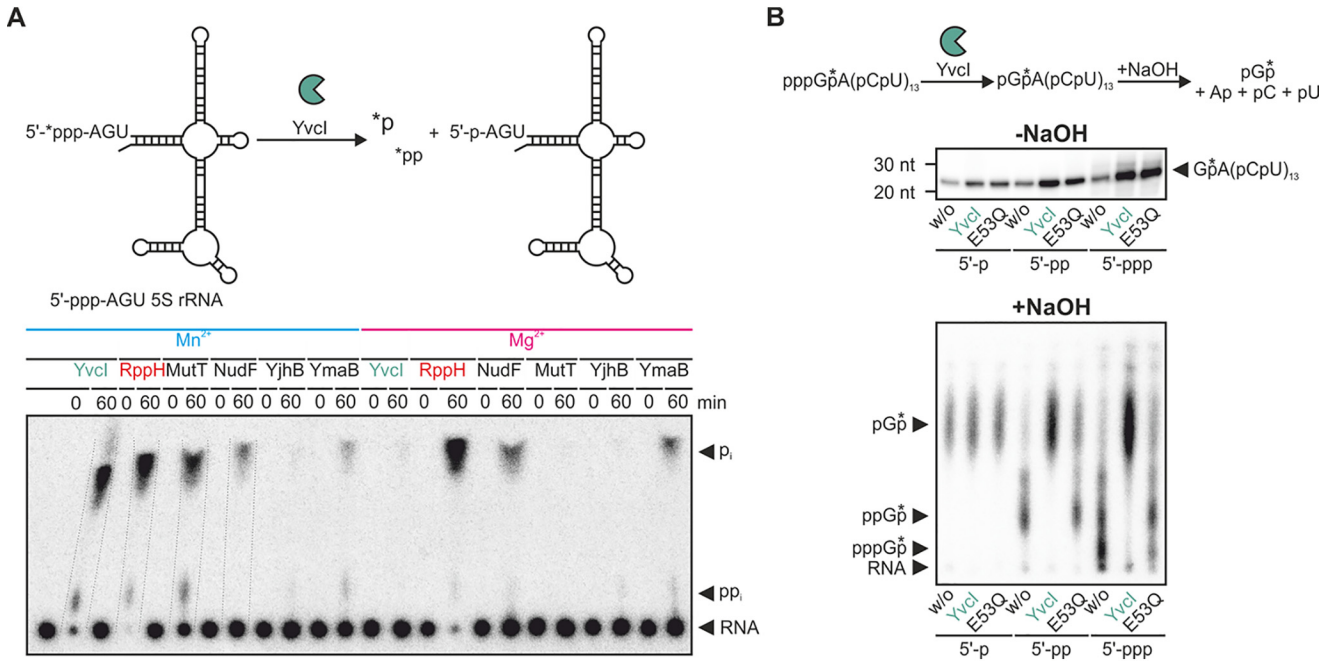

Figure 1. Phosphate removal from 5′-ppp-RNA is catalyzed by several Nudix hydrolases. *A*, ppp-RNA (AGU 5S rRNA, 5′-labeled, 0.5 μM) was incubated with YvcI, BsRppH, MutT, NudF, YjhB, or YmaB (2 μM each, 0.1 μM for BsRppH) in 1× magnesium buffer or 1× manganese buffer (2 mM Mg^{2+} or Mn^{2+}). PEI-cellulose TLC, phosphorimaging of radioactivity. *B*, conversion of 5′-ppp- and 5′-pp-RNA to 5′p-RNA by YvcI. p/p/p-RNA (p-, pp-, and ppp-GA$(CU)_{13}$, with the ^{32}P as part of the phosphate (*) between the first and the second nucleotide) was incubated without (*w/o*) or with YvcI or YvcI-E53Q (2 μM) in 1× manganese buffer (2 mM Mn^{2+}). The reaction products were subjected to alkaline hydrolysis (*lower panel*) or not (*upper panel*). Analysis for samples hydrolyzed with NaOH was performed as for *A*, and for nonhydrolyzed samples, we used 15% PAGE and phosphorimaging of radioactivity.

according to Ref. 11), whereas the nucleotide at the +3 and +4 positions are of minor influence (11, 12). This pronounced substrate specificity of BsRppH and the observation that crude cell extracts of Δ*rppH* cells still show pyrophosphohydrolase activity suggested the existence of at least one additional RNA pyrophosphohydrolase in *B. subtilis* (9). The unknown enzyme is assumed to show much lesser substrate specificity than BsRppH (11, 12). However, the RNA pyrophosphohydrolase activity of candidate enzymes was only investigated *in vitro* in the presence of magnesium ions (9).

Recently we observed that BsRppH can hydrolyze the pyrophosphate bond in NAD-capped RNA much more efficiently when the divalent cation is exchanged from Mg^{2+} to Mn^{2+} (13). *B. subtilis* is a well-studied model for the coordinated regulation of manganese homeostasis (14), and several Nudix hydrolases are known to accept or require manganese as a cofactor (reviewed in Ref. 13). These precedents prompted us to reinvestigate several of the poorly characterized Nudix hydrolases from *B. subtilis*, YvcI, NudF, MutT, YjhB, and YmaB, for their RNA pyrophosphohydrolase activity in the presence of magnesium (Mg^{2+}) and manganese (Mn^{2+}) ions. YvcI, as a novel RNA pyrophosphohydrolase, was studied *in vitro* with respect to its substrate requirements, metal ion and pH dependence. In addition, we show that the Nudix motif of YvcI is the catalytic site for phosphate removal.

Results

Several Nudix hydrolases from B. subtilis remove terminal phosphate groups from 5′-ppp-RNA in vitro

The six candidate hydrolases from *B. subtilis* were assayed for their capability to remove phosphate groups from 5′-ppp-RNA *in vitro* with either Mn^{2+} or Mg^{2+} (Fig. 1*A*). All proteins were prepared as C-terminally His_6-tagged versions, and MutT and YjhB were expressed as maltose-binding protein fusions to increase their solubility. The structurally defined 5S rRNA (5′-labeled with [γ-^{32}P]ATP) was used as substrate, whereby three unpaired nucleotides (AGU) were appended at its 5′-terminus. Using this substrate, all enzymes (with the exception of YjhB, which was completely inactive) preferentially released orthophosphate rather than pyrophosphate. For BsRppH, NudF, and YmaB, the release of γ-^{32}P proceeded independent of the nature of the metal ion, whereas YvcI and MutT released [γ-^{32}P]p_i only (or with much higher efficiency) with manganese as cofactor. The Mn^{2+}-dependent activity or inactivity of these enzymes was confirmed with a different substrate, namely a 5′-terminal fragment of the *gapB* mRNA (Fig. S1*A*).

Because the RNA pyrophosphohydrolase activity of YvcI showed this peculiar metal ion dependence and because YvcI was the most active hydrolase other than BsRppH, it was studied in detail. To determine the preferred phosphorylation state of the enzyme's substrates and products, a RNA oligomer ($GA(CU)_{13}$ (2)) was generated, having either a monophosphate, diphosphate, or triphosphate at the 5′-terminus and ^{32}P at the phosphate between the first and second nucleotide. After treatment with YvcI, the reaction product was hydrolyzed using NaOH and the 5′-terminal phosphorylated nucleotide analyzed by TLC (Fig. 1*B*). Both 5′-pp$GA(CU)_{13}$ and 5′-ppp$GA(CU)_{13}$ were converted by YvcI into 5′-p$GA(CU)_{13}$, which was detected as radiolabeled pGp following alkaline hydrolysis. No ppGp was produced from 5′-ppp$GA(CU)_{13}$. A YvcI mutant with an Glu to Gln exchange at position 53 of the Nudix

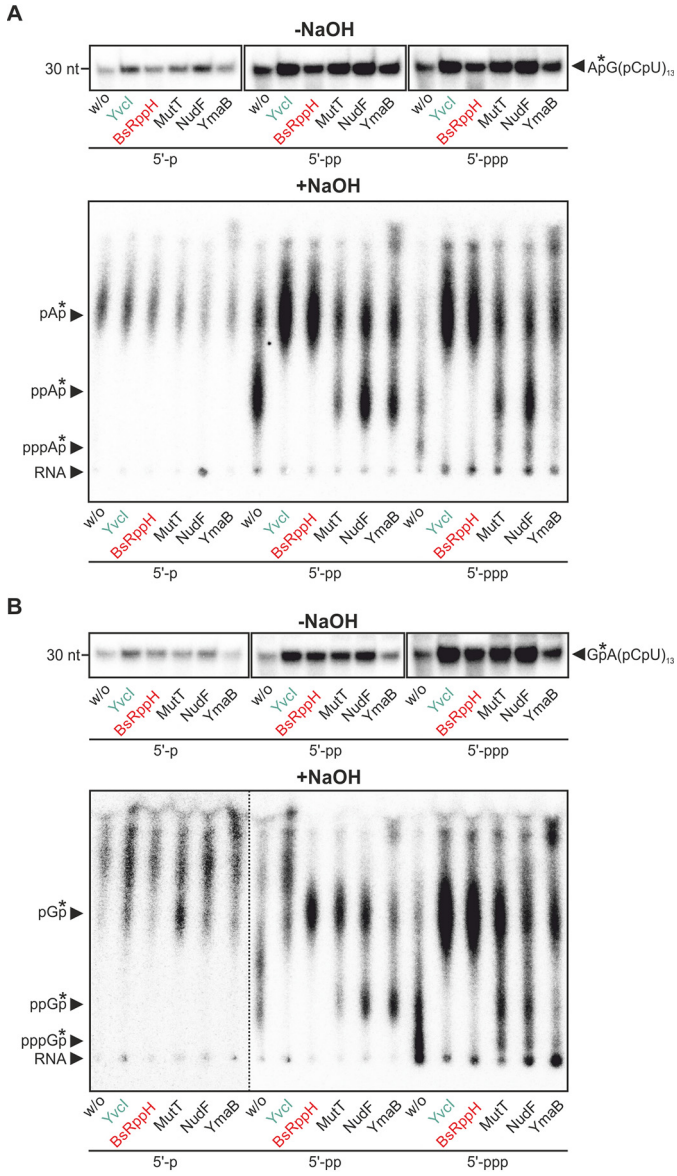

Figure 2. RNA pyrophosphohydrolase activity of Nudix hydrolases from *B. subtilis*. *A* and *B*, conversion of 5′-ppp- and 5′-pp-RNA to 5′p-RNA by YvcI, BsRppH, MutT NudF, and YmaB. p/p/p-RNA (p-, pp-, and ppp-AG(CU)13 (*A*) and p-, pp-, and ppp-GA(CU)13 (*B*), with the ^{32}P as part of the phosphate (*) between the first and the second nucleotide) was incubated in absence (*w/o*) or presence of the Nudix hydrolases, respectively (2 μM each; 0.1 μM for BsRppH) in 1× manganese buffer (2 mM Mn^{2+}). The reaction products were subjected to alkaline hydrolysis (*lower panel*) or not (*upper panel*). Analysis for samples hydrolyzed with sodium hydroxide by PEI-cellulose TLC and for nonhydrolyzed samples by 15% PAGE, phosphorimaging of radioactivity. The *dotted line* indicates where different parts of the same plate, in which the contrast was adjusted separately, were combined to facilitate interpretation.

motif showed a severely compromised activity. RNA substrates 5′-ppAG(CU)$_{13}$ and 5′-pppAG(CU)$_{13}$ were similarly converted into 5′-p-RNA by YvcI (Fig. S1*B*).

In addition, BsRppH, MutT, NudF and YmaB were tested on 5′-(p)ppGA(CU)$_{13}$ and 5′-(p)ppAG(CU)$_{13}$ RNA in Mn^{2+} buffer (Fig. 2). BsRppH quantitatively converted all substrates into p-RNA, independent of the initiating nucleotide, whereas MutT and NudF catalyzed the reaction incompletely. YmaB was more active on the ppp-RNA substrates in this experiment.

Comparison of YvcI to other Nudix hydrolases and determination of its metal cofactor specificity

In contrast to BsRppH, *E. coli* RppH (EcRppH) releases the terminal phosphate groups primarily as pp$_i$ *in vitro* (2). Comparison of the reaction products of AGU 5S treated with YvcI, BsRppH, and EcRppH revealed that YvcI behaves unlike EcRppH and like BsRppH (Fig. 3). Quantitative phosphate removal was achieved by p$_i$ release (>84%; ~14% pp$_i$), whereas only ~5% of the radiolabel was released as p$_i$ in case of EcRppH. BsRppH and EcRppH did not show any difference in their activity when Mn^{2+} was exchanged by Mg^{2+}, whereas YvcI was only active with manganese. Monitoring the course of the enzymatic phosphate release revealed the following order of activity: BsRppH > YvcI > MutT > NudF > YmaB (Fig. S2). Under multiple turnover conditions, BsRppH was much more active than YvcI *in vitro* (Fig. S3, *A* and *B*). A comparative study of the effect of different divalent cations (Zn^{2+}, Cu^{2+}, Mn^{2+}, Mg^{2+}, and Ca^{2+}) on the hydrolysis of 5′-radiolabeled ppp-AGU 5S rRNA by YvcI revealed that the enzyme released the γ-^{32}P only in the presence of manganese (Fig. S3*C*).

The presence of magnesium does not impede YvcI, which acts as homotetramer in solution and has a slightly acidic pH optimum

In cells, metal ions are present in the cytosol at different concentrations. In *B. subtilis*, the intracellular concentration of manganese is buffered to a low micromolar range (15), whereas Mg^{2+} is in the low millimolar range (16). Because no phosphate removal from ppp-RNA by YvcI was observed with magnesium alone, it was tested whether magnesium might nevertheless impair the manganese-dependent enzymatic activity of YvcI (Fig. S3, *D–G*). Between 10 and 100 μM Mn^{2+}, no phosphate removal was observed (Fig. S3, *D* and *F*). At 1 mM Mn^{2+}, ~50% of the ppp-RNA was dephosphorylated after 1 h under the applied conditions. 2 mM Mn^{2+} or more (5 mM) enabled YvcI to efficiently dephosphorylate the ppp-RNA quantitatively (5 mM Mn^{2+}) or nearly quantitatively (~20% remaining ppp-RNA; 2 mM Mn^{2+}) already after 10 min. The RNA was stable under all conditions, ruling out nonspecific degradation of the oligonucleotide (Fig. S3*E*). When magnesium was added to the reaction mixture at a concentration of 2 mM, dephosphorylation was slightly impaired in the presence of 1 mM Mn^{2+} but restored to normal at 2 mM Mn^{2+} (Fig. S3*G*). This indicated that the presence of physiological concentrations of magnesium do not, or only to a negligible extent, impair phosphate removal from ppp-RNA by YvcI *in vitro* as long as the manganese concentration is equal to or greater than 2 mM.

Next, the dephosphorylation reaction was studied by varying the YvcI–RNA ratio and constituting single- or multiple turnover conditions (Fig. 4). Phosphate removal, ~78% as p$_i$ and ~11% as pp$_i$ after 1 h, from the ppp-RNA was efficiently catalyzed by YvcI when the enzyme (monomer) was added in 4-fold excess over the RNA (Fig. 4, *A–C*). At lower RNA– enzyme ratios, p$_i$ removal was decelerated and became rather inefficient under multiple-turnover condi-

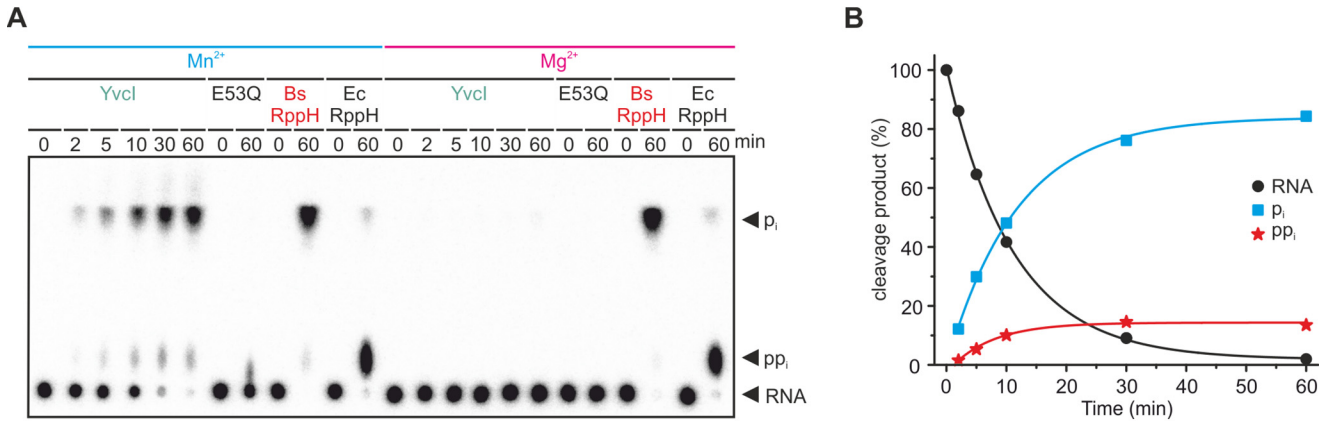

Figure 3. YvcI releases mostly orthophosphate from 5′-ppp-RNA in the presence of manganese. *A*, ppp-RNA (AGU 5S rRNA, 5′-labeled, 0.5 μM) was incubated with YvcI, YvcI-E53Q, BsRppH, or EcRppH (2 μM each, 0.1 μM for Bs/EcRppH) in 1× manganese buffer or 1× magnesium buffer. PEI-cellulose TLC, phosphorimaging of radioactivity is shown. *B*, quantification of the Mn^{2+}-dependent time trace of YvcI depicted in *A*.

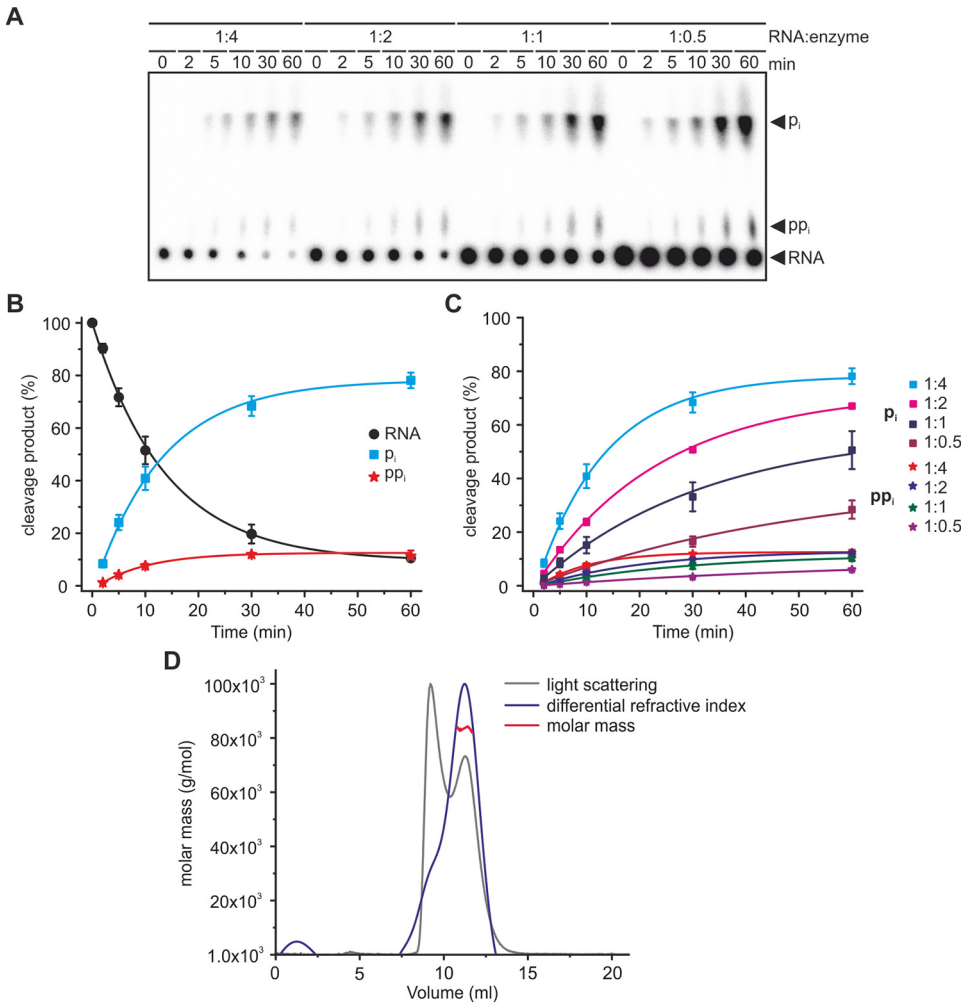

Figure 4. Titration of RNA. *A*, 4-fold surplus of YvcI (monomer) over the RNA substrate is needed for efficient catalysis. ppp-RNA (AGU 5S rRNA, 5′-labeled) was incubated with YvcI (2 μM) in 1× manganese buffer (2 mM Mn^{2+}). The RNA–enzyme ratio is as indicated. PEI-cellulose TLC, phosphorimaging of radioactivity is shown. *B* and *C*, quantification of ppp-RNA, p_i, and pp_i from *A*. *B*, quantification of the cleavage products at an RNA–enzyme ratio of 1:4, showing means ± S.D. of two independent experiments (technical replicates). *C*, quantification of p_i and pp_i. The RNA–enzyme ratio is indicated. Statistics are as for *B*. *D*, multiangle light-scattering analysis indicates YvcI to be a tetramer in solution. The scattered light (*gray*) and the protein concentration (*blue*) were used to determine the molar mass distribution (*red*) along the YvcI elution peak.

tions (8-fold slower at an RNA–enzyme ratio of 1:0.5). Multiangle light-scattering analysis indicated that the enzyme exists predominantly as a homotetramer in solution (Fig. 4*D*).

Many of the Nudix hydrolases have alkaline pH optima (17), among them also BsRppH (pH optimum of 8.5 to 9) (18) and NudC from *E. coli* (pH optimum of 8) (19). In contrast to BsRppH, YvcI was more active at neutral to slightly acidic pH and

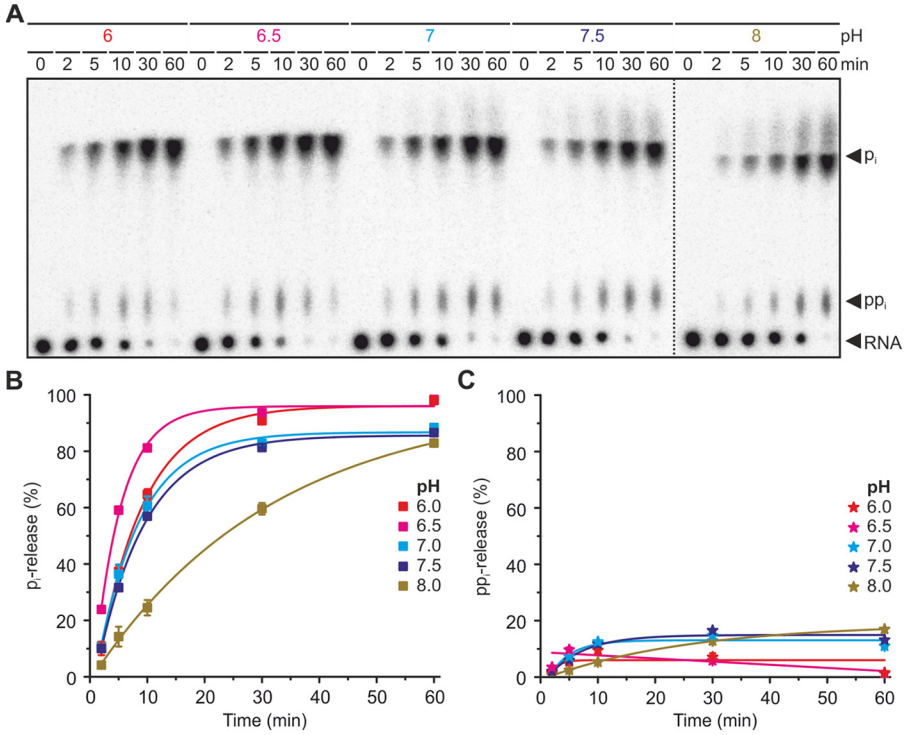

Figure 5. pH dependence of the phosphate removal from ppp-RNA catalyzed by YvcI. *A*, YvcI is most active under slight acidic to neutral pH. ppp-RNA (AGU 5S rRNA, 5′-labeled, 0.5 μM) was incubated with YvcI (2 μM) in 1× manganese buffer (2 mM Mn^{2+}). The *dotted line* indicates where different parts of different plates were combined to facilitate interpretation. PEI-cellulose TLC, phosphorimaging of radioactivity is shown. *B* and *C*, quantification of orthophosphate (p_i) (*B*) and pyrophosphate (pp_i) (*C*) from *A*, showing means ± S.D. of two independent experiments (technical replicates).

had an optimum at pH 6.5 (Fig. 5). Interestingly, at pH 8 the amount of released pp_i (~17%) was 10-fold higher than the amount released at pH 6 (~1.6%).

The Nudix motif of YvcI is responsible for phosphate removal from ppp-RNA

The Nudix motif is generally the active site of Nudix hydrolases (20). As seen for BsRppH, especially the glutamate residues in the active site are important for phosphate removal of ppp-RNA (9, 12) and decapping of NAD-RNA (13). To elucidate whether the Nudix motif is also the active site of YvcI, mutants with amino acid exchanges of the putatively important glutamate residues were prepared by site-directed mutagenesis (Fig. S4*A*) and tested for their ability to dephosphorylate ppp-AGU 5S rRNA (Fig. 6 and Fig. S4*B*) and two mRNAs (Fig. S5). Replacement of the glutamate residues 49 and 53 nearly quantitatively (~5% p_i) or quantitatively (<1% p_i) abolished the enzymatic activity. In contrast, the activity of the YvcI-E52Q mutant was only slightly compromised compared with the WT (Fig. 6*A*). When E52Q was combined with either E49Q or E53Q in double mutants (Fig. S4*A*, *right panel*), none of these mutants was active (Fig. 6*A*). In addition, all mutants were inactive in Mg^{2+} buffer (Fig. 6*B*).

The nucleotides at position +1 and +2 of the RNA influence the activity of YvcI

Usually, either adenosine (A) or guanosine (G) nucleosides occupy the 5′-end of primary transcripts in bacteria. Because the terminal nucleotide is likely to make intimate contact with the active site of YvcI, the sequence preference of the enzyme was studied using an RNA with a defined tertiary structure. Specifically, 5S rRNA with three unpaired nucleotides at its 5′-end, with either an A or a G at its 5′-end, was used as substrate (Fig. 7). YvcI accepted and removed phosphate from both RNAs. Notably, the RNA with a terminal guanosine was dephosphorylated ~6-fold faster than its counterpart with a 5′-A. This finding contrasts the substrate specificity of BsRppH, which slightly prefers A-initiating RNAs (11). U- or C-initiating 5S RNA variants were not tested because only very few promotors initiate with a pyrimidine nucleotide in bacteria (21).

Next, the identity of the second nucleotide (+2) was varied and its effect on the reactivity of YvcI studied (Fig. 8). In case of 5S rRNA starting with an adenosine, U at position +2 was best, whereas the rate differences between the other three variants were insignificant. For variants initiating with G, the nucleotide at position +2 effected the dephosphorylation in the following order: G > U > A ~ C. This observation is in contrast to BsRppH, which efficiently dephosphorylates only RNAs with a guanosine at position +2, irrespective of the RNA initiating with an A or a G (11, 12).

5′-RNA ends influence efficiency and product composition of YvcI's RNA pyrophosphohydrolysis

For BsRppH, the secondary structure at the 5′-end of the RNA has been found to matter (11). To study this phenomenon for YvcI, variants of the 5S rRNA initiating with G were prepared with an unambiguous secondary structure having either a blunt end, a single unpaired nucleotide at the 3′-end or one, two, three, or four unpaired nucleotides at the 5′-end (Fig. 9, *A–C*). With an increasing number of 5′-unpaired nucleotides,

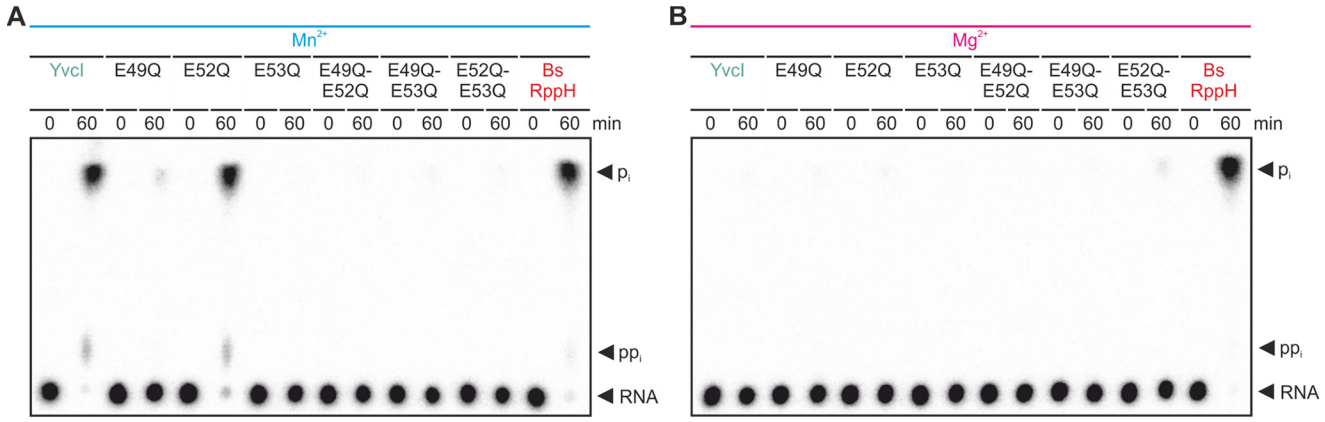

Figure 6. Effects of YvcI amino acid exchanges in the Nudix motif on the RNA pyrophosphohydrolase activity. ppp-RNA (AGU 5S rRNA, 5′-labeled, 0.5 μM) was incubated with YvcI (mutants) (2 μM) in 1× manganese buffer (*A*) or 1× magnesium buffer (*B*). PEI-cellulose TLC, phosphorimaging of radioactivity is shown.

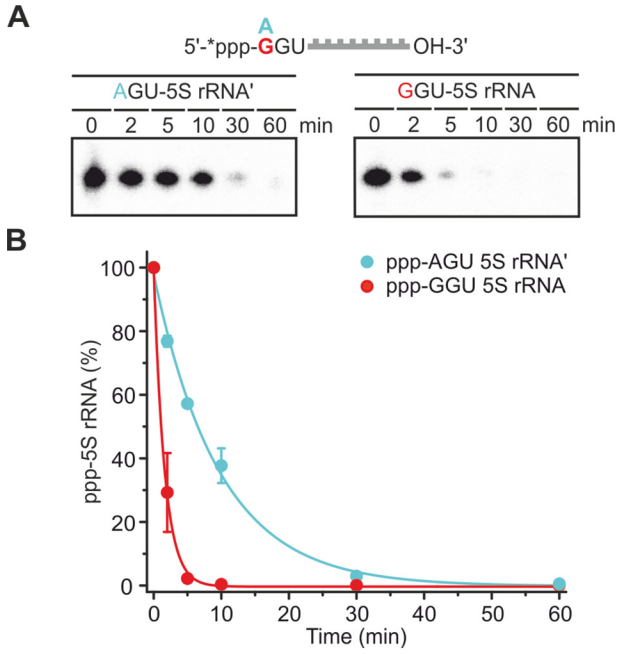

Figure 7. Influence of the +1 position of RNA on phosphate removal by YvcI. *A*, ppp-RNA (XGU 5S rRNA, 5′-labeled (*), 0.5 μM) was incubated with YvcI (2 μM) in 1× manganese buffer. 8% PAGE, phosphorimaging of radioactivity is shown. *B*, quantification of the ppp-RNA from *A*, showing means ± S.D. of three independent experiments (technical replicates).

phosphate removal was increased ~7-fold (+1 unpaired 5′-nucleotide), ~13-fold (+2), ~25-fold (+3), or ~32-fold (+4) compared with the substrate with a blunt end. The addition of one nucleotide at the 3′-end additionally decelerated the reaction by ~6-fold. Strikingly, in any case more pp_i was released than p_i. When the analogous 5S rRNAs initiating with an A were tested, again more p_i than pp_i was released (Fig. 9, *D–F*). Thereby, the effect of the 5′-overhang was not as pronounced as for the 5′-G initiating RNAs. Compared with the blunt end substrate, phosphate removal was increased ~2–4-fold (+4) with the RNA having three unpaired nucleotides at the 5′-terminus being the favored substrate.

These findings illustrate that YvcI behaves similar to EcRppH (4) and BsRppH (11) and needs at least one and prefers two or more unpaired nucleotides at the 5′-end of its substrate. The peculiar observation that the nature of the terminal nucleotide determines whether majorly ortho- or pyrophosphate is released has, to the best of our knowledge, not yet been described in literature.

YvcI removes terminal phosphate groups from mRNAs in vitro but does not accept NAD-RNA as substrate

Because processed 5S rRNA bears a monophosphate at its 5′-end, it is unlikely to be an *in vivo* substrate of YvcI. However, its defined secondary structure rendered it a suitable substrate to study the substrate requirements of YvcI. Following the initial studies, native mRNAs were tested as substrates (Fig. 10 and Fig. S6). YvcI accepted *veg* mRNA, which has AGU as 5′-end (22), and released the terminal phosphates of the triphosphorylated mRNA (Fig. 10) as ortho- and pyrophosphate. As observed before for the exchange of Glu^{49} by Q (Fig. 6*A*), an exchange of the glutamate by alanine did not fully abolish the dephosphorylating activity of the Nudix hydrolase. Analysis of the reaction kinetics by PAGE (Fig. 10, *B* and *C*) confirmed the results obtained by TLC analysis (Fig. 10*A*).

Two further mRNAs were tested as substrates of YvcI: *csbD* (23) and *ywjC* mRNA (24) (Fig. S6). Both mRNAs were accepted by YvcI as substrate, and phosphate was removed. The two mRNAs initiate with A, whereby the +2 (+3) position of the *csbD* mRNA occupied by a C (A) and a U (A) is present in case of *ywjC* mRNA. *csbD* was slightly faster dephosphorylated (~1.5-fold) than the *veg* mRNA (Fig. 10, *B* and *C*). In contrast, from *ywjC* mRNA phosphate was removed ~5 and ~3.5 times slower than from *csbD* and *veg*, respectively. In addition, ~30% of the ppp-*ywjC* mRNA remained triphosphorylated after 1-h treatment. The accessibility of the 5′-ends of the three tested mRNAs to YvcI might explain the observed differences in phosphate removal.

Because NAD has recently been found to be a cap-like 5′-RNA modification of mRNAs in *B. subtilis* (13), YvcI was tested for its ability to decap NAD-*veg* mRNA (Fig. 10*D*). ^{32}P-NAD-labeled *veg* mRNA with the ^{32}P (*p) at the penultimate phosphate (Np*pA-RNA) was incubated with YvcI in the presence of either Mg^{2+} or Mn^{2+}. Subsequently, the reaction mixture was treated by nuclease P1, which cleaves all phosphodiester bonds within an RNA and would release labeled AMP

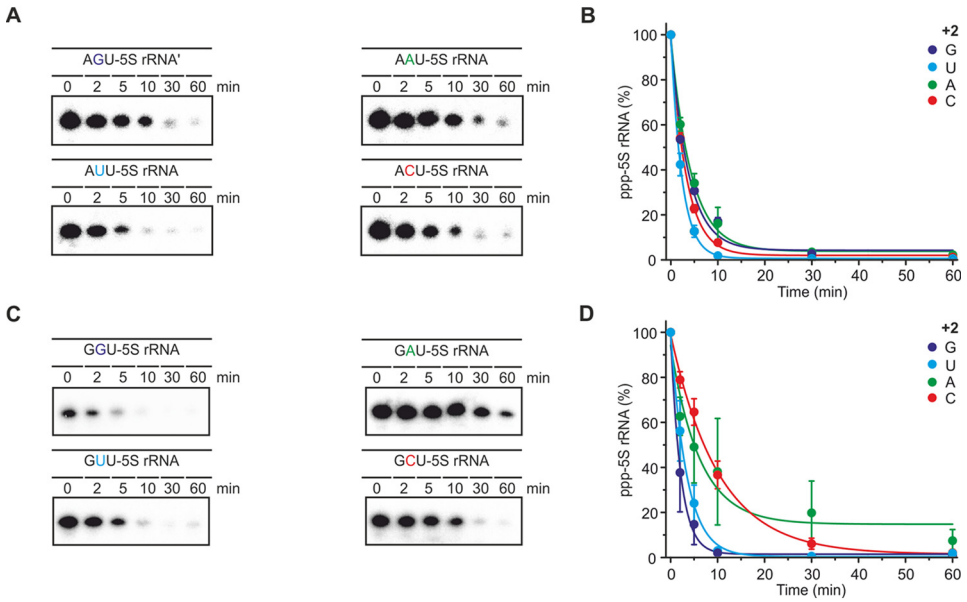

Figure 8. Influence of the +2 position of RNA on phosphate removal by YvcI. *A*, ppp-RNA (A*X*U 5S rRNA, 5′-labeled, 0.5 μM) was incubated with YvcI (2 μM) in 1× manganese buffer, where *X* indicates G, U, A, or C. 8% PAGE, phosphorimaging of radioactivity is shown. *B*, quantification of the ppp-RNA from *A*, showing means ± S.D. of two independent experiments (technical replicates). *C*, description as for *A* but with G*X*U 5S rRNA and YvcI (1 μM). *D*, statistics are as in *B*.

(*pA) if YvcI has cleaved off NMN. *E. coli* NudC, known to decap NAD-RNA (19, 25), served as control. The reaction products were resolved by TLC. YvcI was not capable of decapping NAD-*veg* mRNA under any of the applied conditions.

Discussion

Removal of the γ- and β-phosphate from 5′-triphosphate RNA is the trigger for 5′-monophosphate-dependent RNA decay in bacteria (1). Here, we have identified YvcI, MutT, NudF, and YmaB as novel RNA pyrophosphohydrolases. The most active one, YvcI, was characterized biochemically, and its substrate specificity was determined *in vitro*. The RNA pyrophosphohydrolase activity previously observed in crude extracts of Δ*rppH* cells (9) might therefore be a combined activity of YvcI and the above mentioned Nudix hydrolases. The fact that up to five Nudix hydrolases are able to dephosphorylate ppp-RNA *in vitro* provides another example for the substrate multispecificity and redundancy of this enzyme class (17, 26).

Screening for additional RNA pyrophosphohydrolases among the Nudix hydrolases of *B. subtilis* was already performed by others (9). Here, replacement of the metal ion cofactor Mg^{2+} by Mn^{2+} revealed the ability of four additional Nudix hydrolases in addition to BsRppH to convert triphosphate RNA 5′-ends to monophosphate ends, releasing mixtures of pyrophosphate and orthophosphate (Fig. 1*A*). YvcI and YmaB were found to produce monophosphate RNA 5′-ends with no intermediary diphosphate RNA detected. In contrast, MutT and NudF produced a mixture of monophosphate and diphosphate RNA indicating sequential release of orthophosphate. However, the 5′-diphosphate as novel terminal RNA phosphorylation state has only been identified in *E. coli* (3), and it remains to be determined whether these species exist in *B. subtilis* as well. In that case, MutT and NudF might participate in their formation.

YvcI as novel RNA pyrophosphohydrolase catalyzed efficient phosphate removal at millimolar manganese concentration *in vitro* (Fig. S3, *C–F*). Thereby, millimolar magnesium did not impede catalysis (Fig. S3*G*). This behavior is known from the decapping of m^7G-capped RNA by human Dcp2 (hDcp2) (27). Together with hDcp2, yeast Dcp2, *Xenopus* X29, its human homolog Nudt16, and the NADH pyrophosphatase from *Arabidopsis thaliana*, YvcI forms a group of Nudix hydrolases that prefer Mn^{2+} over Mg^{2+} as cofactor. The intracellular concentration of manganese is reported to reach up to 0.5 mM, and *B. subtilis* tolerates up to 1 mM Mn^{2+} in its environment (14). However, it remains to be determined whether these circumstances enable YvcI to catalyze the reaction *in vivo*. The Nudix motif of YvcI is responsible for catalysis (Fig. 6). The catalytic activity of point mutants is very similar to BsRppH (12). Hence, we speculate that YvcI's Glu^{49} and Glu^{53} carry out a role in the coordination of the manganese ion(s) similar to that of the equivalent glutamates in BsRppH.

The substrate requirements of YvcI and BsRppH differ with respect to the +1 position and +2 position of the RNA. YvcI prefers RNAs initiating with a G (Fig. 7), whereas BsRppH shows a very slight preference for A (11). Moreover, a G at position +2 is preferred by BsRppH for efficient dephosphorylation (11, 12) and facilitates decapping of NAD-RNA by BsRppH (13). In contrast, for YvcI, the nature of the nucleotide at position +2 is almost irrelevant for RNAs starting with A (Fig. 8*A*), whereas slight preferences (G > U > A/C) are observed for RNAs initiating with G (Fig. 8*B*). More similar behavior of YvcI to BsRppH was observed regarding the requirement of the enzymes for unpaired nucleotides at the 5′-terminus with the slight difference that YvcI only needs one nucleotide that is not

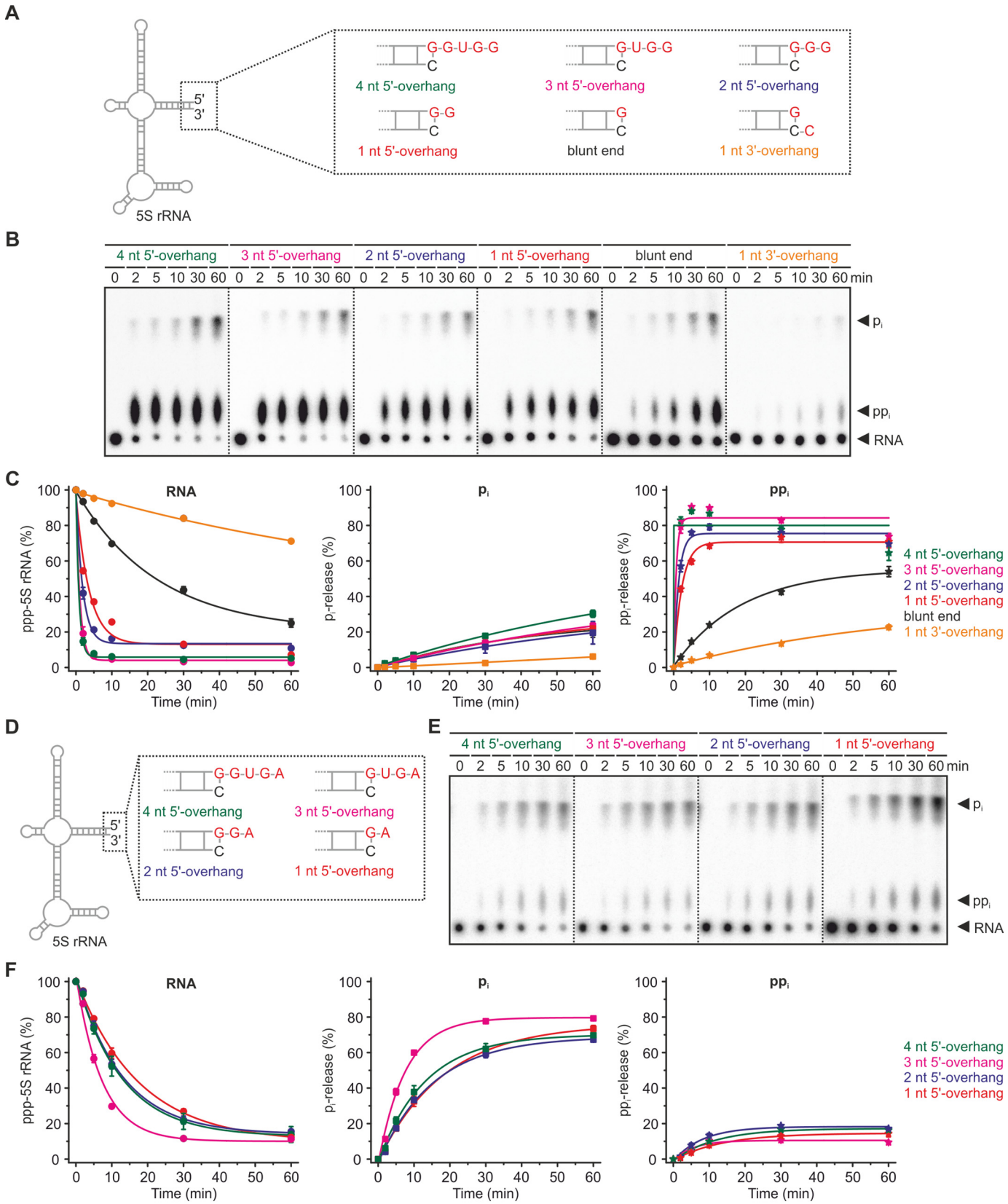

Figure 9. Influence of RNA secondary structure on YvcI's RNA pyrophosphohydrolase activity. *A* and *D*, schemes of 5′-ppp-5S rRNA with different 5′- and 3′-termini initiating either with G (*A*) or A (*D*). *B* and *E*, ppp-RNA (ppp-5S rRNA, 5′-labeled, 0.5 μM) was incubated with YvcI (2 μM) in 1× manganese buffer. PEI-cellulose TLC, phosphorimaging of radioactivity is shown. *C* and *F*, quantification of the ppp-RNA from *B* and *E*, showing means ± S.D. of three independent experiments (technical replicates).

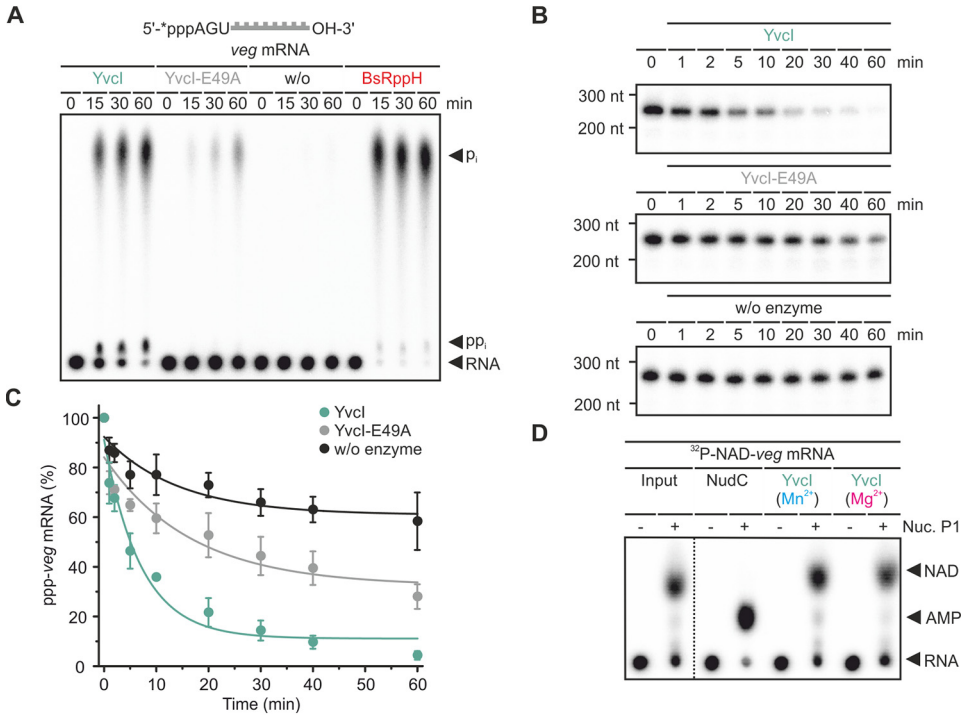

Figure 10. YvcI removes phosphate from ppp-veg mRNA *in vitro*. *A*, ppp-veg mRNA (5′-labeled (*), 0.5 μM) was incubated with YvcI, YvcI-E49A (2 μM each), and BsRppH (0.1 μM) in 1× manganese buffer (1× magnesium buffer for BsRppH). PEI-cellulose TLC, phosphorimaging of radioactivity is shown. *B*, experimental procedure and description as for *A*. 8% PAGE, phosphorimaging of radioactivity is shown. *C*, quantification of the ppp-veg mRNA from *B*, showing means ± S.D. of three independent experiments (technical replicates). *D*, ^{32}P-NAD-veg mRNA (5′-labeled, 4 μM) was incubated with YvcI (1 μM) or NudC (1 μM) in 1× magnesium or 1× manganese buffer. Half of the samples was subsequently treated with Nuclease P1 (*Nuc. P1*, 1 unit). The *dotted line* indicates where different parts of the same plate were combined to facilitate interpretation. PEI-cellulose TLC, phosphorimaging of radioactivity is shown.

sequestered by base pairing for phosphate removal (Fig. 9). BsRppH needs at least two and prefers three or more (11). The most striking feature of YvcI and biggest difference from BsRppH is the observation that the terminal nucleotide (A *versus* G) determines whether majorly ortho- or pyrophosphate is released. This finding might influence the fate of YvcI substrates with respect to processing and turnover. Furthermore, YvcI was found to be inactive on NAD-RNA (Fig. 10*D*). Hence, at least *in vitro*, YvcI and BsRppH seem to partly complement each other regarding their RNA substrates.

Overall our results raise the possibility that YvcI is (one of) the unidentified RNA pyrophosphohydrolase(s) from *B. subtilis*. However, it remains to be determined whether BsRppH is the only RNA pyrophosphohydrolase in the firmicute or whether the other Nudix hydrolases YvcI, MutT, NudF, and YmaB join this family by executing phosphate removal from primary transcripts also *in vivo*. *In vivo* studies have to include investigations on the 5′-p-RNA/5′-ppp-RNA ratio (*e.g.* PABLO assay (28)) and the decay rate of RNAs in respective deletion strains. Moreover, because the *in vitro* RNA pyrophosphohydrolase activity of YvcI was low compared with BsRppH, it will be interesting to elucidate interacting partners that influence its activity. In *E. coli*, the diaminopimelate epimerase DapF (29) has been found to bind to and stimulate the activity of RppH (30). Stimulation by another protein may also alleviate the millimolar Mn^{2+} ion requirement for efficient hydrolysis or binding of YvcI to mRNA targets (as seen for Edc1/2p (31)) and might render the RNA pyrophosphohydrolase more active *in vivo*.

Experimental procedures

Bacterial strains, oligomers, and plasmids

Bacterial strains used in this work are listed in Table S1. All DNAs oligomers (Tables S2 and S3) were purchased from IDT. All chemicals were purchased from Merck if not stated otherwise. All plasmids used for and prepared for this work are listed in Table S4.

Preparation of radiolabeled oligonucleotides by in vitro transcription

Linear templates for the *in vitro* transcription reactions were prepared by PCR using the DNA oligonucleotides listed in Table S3 and *in vitro* transcription performed as described (13). Radiolabeled ppp-, pp-, and p-GA$(CU)_{13}$ or AG$(CU)_{13}$ oligonucleotides were prepared as described (2). All RNAs were purified by PAGE. Radiolabeled RNA, nucleotides or phosphate on gels, or TLC plates were visualized by phosphorimaging using a Typhoon FLA 9500 imager (GE Healthcare), quantified using ImageQuant software (GE Healthcare) and plotted using OriginPro software (OriginLab Corporation).

YvcI cleavage assays

Different 5′-radiolabeled RNAs in 1× manganese buffer (50 mM Tris-HCl, pH 7.5, 2 mM $MnCl_2$, 1 mM DTT) or 1× magnesium buffer (50 mM Tris-HCl, pH 7.5, 2 mM $MgCl_2$, 1 mM DTT) were incubated with Nudix hydrolases (mutants) at 37 °C for up to 60 min. Tris-HCl was exchanged by Bis-Tris-methane (pH 6.0/6.5) to prepare the 1× manganese buffer used in the pH

study. Magnesium or manganese, respectively, was replaced by zinc (Zn^{2+}), copper (Cu^{2+}), or calcium (Ca^{2+}) where indicated. The reaction products were analyzed by PAGE or TLC. TLC analysis for the separation of RNA, orthophosphate, and pyrophosphate was performed using polyethyleneimine (PEI)-cellulose plates (Merck) (prerun with water and air-dried) in 0.75 M LiCl (32) or 0.3 M phosphate buffer, pH 6.3, with 20% methanol combining approaches described in Refs. 2 and 33). Aliquots (7 μl) of the reaction mixtures were quenched with 50 mM EDTA, pH 8 (4 μl), and stored at −20 °C until TLC analysis. Samples (10 μl) of the radiolabeled $GA(CU)_{13}$ or $AG(CU)_{13}$ oligonucleotide ribonucleotides treated with YvcI, YvcI-E53Q, or no enzyme in 1× manganese buffer at 37 °C for 30 min (60 min for the experiment conducted with various other Nudix hydrolases) were subjected to alkaline hydrolysis by the addition of 5 μl of NaOH (0.2 M) and incubation at 95 °C for 15 min. 5 μl of formic acid (3 M) was added to neutralize the solution, and the reaction products were subjected to PEI-cellulose TLC analysis in 0.75 M KH_2PO_4, pH 3.65 (34). Aliquots of ^{32}P-NAD-RNA treated with YvcI, NudC, or no enzyme in 1× manganese buffer or 1× magnesium buffer II (25 mM Tris, pH 7.5, 50 mM NaCl, 50 mM KCl, 10 mM $MgCl_2$, 1 mM DTT) (25), respectively, at 37 °C for 30 min were then treated with 0.1 unit/μl Nuclease P1 (Merck) in 50 mM NH_4-acetate, pH 5.5, at 37 °C for 30 min with subsequent incubation at 70 °C for 10 min. The reaction products were resolved by PEI-cellulose TLC in 1 M NH_4-acetate pH5.5/ethanol (ratio, 4:6) as described (13).

Author contributions—J. F. and A. J. conceptualization; J. F., M. A. K., and Y. Z. data curation; J. F., I. S., and A. J. formal analysis; J. F. validation; J. F., M. A. K., Y. Z., Y.L.A., and I. S. investigation; J. F., M. A. K., and Y. Z. visualization; J. F., M. A. K., and Y.L.A. methodology; J. F. writing-original draft; J. F., M. A. K., Y. Z., Y.L.A., I. S., and A. J. writing-review and editing; A. J. supervision; A. J. funding acquisition.

Acknowledgments—We thank Leonie Kolmar and Christina Hacker for experimental assistance and members of the Jäschke lab for fruitful discussions.

References

1. Hui, M. P., Foley, P. L., and Belasco, J. G. (2014) Messenger RNA degradation in bacterial cells. *Annu. Rev. Genet.* **48,** 537–559 CrossRef Medline
2. Deana, A., Celesnik, H., and Belasco, J. G. (2008) The bacterial enzyme RppH triggers messenger RNA degradation by 5′ pyrophosphate removal. *Nature* **451,** 355–358 CrossRef Medline
3. Luciano, D. J., Vasilyev, N., Richards, J., Serganov, A., and Belasco, J. G. (2017) A novel RNA phosphorylation state enables 5′ end-dependent degradation in *Escherichia coli*. *Mol. Cell* **67,** 44–54.e6 CrossRef Medline
4. Foley, P. L., Hsieh, P. K., Luciano, D. J., and Belasco, J. G. (2015) Specificity and evolutionary conservation of the *Escherichia coli* RNA pyrophosphohydrolase RppH. *J. Biol. Chem.* **290,** 9478–9486 CrossRef Medline
5. Vasilyev, N., and Serganov, A. (2015) Structures of RNA complexes with the *Escherichia coli* RNA pyrophosphohydrolase RppH unveil the basis for specific 5′-end-dependent mRNA decay. *J. Biol. Chem.* **290,** 9487–9499 CrossRef Medline
6. Lehnik-Habrink, M., Lewis, R. J., Mäder, U., and Stülke, J. (2012) RNA degradation in *Bacillus subtilis*: an interplay of essential endo- and exoribonucleases. *Mol. Microbiol.* **84,** 1005–1017 CrossRef Medline
7. Mathy, N., Bénard, L., Pellegrini, O., Daou, R., Wen, T., and Condon, C. (2007) 5′-to-3′ exoribonuclease activity in bacteria: role of RNase J1 in rRNA maturation and 5′ stability of mRNA. *Cell* **129,** 681–692 CrossRef Medline
8. Dorléans, A., Li de la Sierra-Gallay, I., Piton, J., Zig, L., Gilet, L., Putzer, H., and Condon, C. (2011) Molecular basis for the recognition and cleavage of RNA by the bifunctional 5′-3′ exo/endoribonuclease RNase J. *Structure* **19,** 1252–1261 CrossRef Medline
9. Richards, J., Liu, Q., Pellegrini, O., Celesnik, H., Yao, S., Bechhofer, D. H., Condon, C., and Belasco, J. G. (2011) An RNA pyrophosphohydrolase triggers 5′-exonucleolytic degradation of mRNA in *Bacillus subtilis*. *Mol. Cell* **43,** 940–949 CrossRef Medline
10. Durand, S., Gilet, L., Bessières, P., Nicolas, P., and Condon, C. (2012) Three essential ribonucleases—RNase Y, J1, and III—control the abundance of a majority of *Bacillus subtilis* mRNAs. *PLoS Genet.* **8,** e1002520 CrossRef Medline
11. Hsieh, P. K., Richards, J., Liu, Q., and Belasco, J. G. (2013) Specificity of RppH-dependent RNA degradation in *Bacillus subtilis*. *Proc. Natl. Acad. Sci. U.S.A.* **110,** 8864–8869 CrossRef Medline
12. Piton, J., Larue, V., Thillier, Y., Dorléans, A., Pellegrini, O., Li de la Sierra-Gallay, I., Vasseur, J. J., Debart, F., Tisné, C., and Condon, C. (2013) *Bacillus subtilis* RNA deprotection enzyme RppH recognizes guanosine in the second position of its substrates. *Proc. Natl. Acad. Sci. U.S.A.* **110,** 8858–8863 CrossRef Medline
13. Frindert, J., Zhang, Y., Nübel, G., Kahloon, M., Kolmar, L., Hotz-Wagenblatt, A., Burhenne, J., Haefeli, W. E., and Jäschke, A. (2018) Identification, biosynthesis, and decapping of NAD-capped RNAs in *B. subtilis*. *Cell Rep.* **24,** 1890–1901.e8 CrossRef Medline
14. Helmann, J. D. (2014) Specificity of metal sensing: iron and manganese homeostasis in *Bacillus subtilis*. *J. Biol. Chem.* **289,** 28112–28120 CrossRef Medline
15. Ma, Z., Faulkner, M. J., and Helmann, J. D. (2012) Origins of specificity and cross-talk in metal ion sensing by *Bacillus subtilis* fur. *Mol. Microbiol.* **86,** 1144–1155 CrossRef Medline
16. Foster, A. W., Osman, D., and Robinson, N. J. (2014) Metal preferences and metallation. *J. Biol. Chem.* **289,** 28095–28103 CrossRef Medline
17. McLennan, A. G. (2006) The Nudix hydrolase superfamily. *Cell. Mol. Life Sci.* **63,** 123–143 CrossRef Medline
18. Xu, W., Jones, C. R., Dunn, C. A., and Bessman, M. J. (2004) Gene ytkD of *Bacillus subtilis* encodes an atypical nucleoside triphosphatase member of the Nudix hydrolase superfamily. *J. Bacteriol.* **186,** 8380–8384 CrossRef Medline
19. Höfer, K., Li, S., Abele, F., Frindert, J., Schlotthauer, J., Grawenhoff, J., Du, J., Patel, D. J., and Jäschke, A. (2016) Structure and function of the bacterial decapping enzyme NudC. *Nat. Chem. Biol.* **12,** 730–734 CrossRef Medline
20. Bessman, M. J., Frick, D. N., and O'Handley, S. F. (1996) The MutT proteins or "nudix" hydrolases, a family of versatile, widely distributed, "housecleaning" enzymes. *J. Biol. Chem.* **271,** 25059–25062 CrossRef Medline
21. Reddy, P. S., and Chatterji, D. (1994) Evidence for a pyrimidine-nucleotide-specific initiation site (the i site) on *Escherichia coli* RNA polymerase: proximity relationship with the inhibitor binding domain. *Eur. J. Biochem.* **225,** 737–745 CrossRef Medline
22. Fukushima, T., Ishikawa, S., Yamamoto, H., Ogasawara, N., and Sekiguchi, J. (2003) Transcriptional, functional and cytochemical analyses of the *veg* gene in *Bacillus subtilis*. *J. Biochem.* **133,** 475–483 CrossRef Medline
23. Akbar, S., Lee, S. Y., Boylan, S. A., and Price, C. W. (1999) Two genes from *Bacillus subtilis* under the sole control of the general stress transcription factor sigma B. *Microbiology* **145,** 1069–1078 CrossRef Medline
24. Presecan, E., Moszer, I., Boursier, L., Cruz Ramos, H., de la Fuente, V., Hullo, M. F., Lelong, C., Schleich, S., Sekowska, A., Song, B. H., Villani, G., Kunst, F., Danchin, A., and Glaser, P. (1997) The *Bacillus subtilis* genome from gerBC (311 degrees) to licR (334 degrees). *Microbiology* **143,** 3313–3328 CrossRef Medline
25. Cahová, H., Winz, M. L., Höfer, K., Nübel, G., and Jäschke, A. (2015) NAD captureSeq indicates NAD as a bacterial cap for a subset of regulatory RNAs. *Nature* **519,** 374–377 CrossRef Medline
26. McLennan, A. G. (2013) Substrate ambiguity among the nudix hydrolases: biologically significant, evolutionary remnant, or both? *Cell. Mol. Life Sci.* **70,** 373–385 CrossRef Medline
27. Piccirillo, C., Khanna, R., and Kiledjian, M. (2003) Functional characterization of the mammalian mRNA decapping enzyme hDcp2. *RNA* **9,** 1138–1147 CrossRef Medline

28. Celesnik, H., Deana, A., and Belasco, J. G. (2008) PABLO analysis of RNA: 5′-phosphorylation state and 5′-end mapping. *Methods Enzymol.* **447,** 83–98 CrossRef Medline
29. Richaud, C., Higgins, W., Mengin-Lecreulx, D., and Stragier, P. (1987) Molecular cloning, characterization, and chromosomal localization of DapF, the *Escherichia coli* gene for diaminopimelate epimerase. *J. Bacteriol.* **169,** 1454–1459 CrossRef Medline
30. Lee, C. R., Kim, M., Park, Y. H., Kim, Y. R., and Seok, Y. J. (2014) RppH-dependent pyrophosphohydrolysis of mRNAs is regulated by direct interaction with DapF in *Escherichia coli*. *Nucleic Acids Res.* **42,** 12746–12757 CrossRef Medline
31. Schwartz, D., Decker, C. J., and Parker, R. (2003) The enhancer of decapping proteins, Edc1p and Edc2p, bind RNA and stimulate the activity of the decapping enzyme. *RNA* **9,** 239–251 CrossRef Medline
32. Liu, S. W., Jiao, X., Welch, S., and Kiledjian, M. (2008) Analysis of mRNA decapping. *Methods Enzymol.* **448,** 3–21 CrossRef Medline
33. Huang, F., and Yarus, M. (1997) Versatile 5′ phosphoryl coupling of small and large molecules to an RNA. *Proc. Natl. Acad. Sci. U.S.A.* **94,** 8965–8969 CrossRef Medline
34. Hwang, J., and Inouye, M. (2001) An essential GTPase, Der, containing double GTP-binding domains from *Escherichia coli* and *Thermotoga maritima*. *J. Biol. Chem.* **276,** 31415–31421 CrossRef Medline